

PAPER • OPEN ACCESS

Film boiling heat transfer from a wire to upward flow of liquid hydrogen and liquid nitrogen

To cite this article: M Shiotsu *et al* 2015 *IOP Conf. Ser.: Mater. Sci. Eng.* **101** 012175

View the [article online](#) for updates and enhancements.

You may also like

- [Fault current limiting HTS transformer with extended fault withstand time](#)
Mohammad Yazdani-Asrami, Mike Staines, Gennady Sidorov et al.
- [Onset of flow instability with one-side heated swirl tube for fusion reactor safety](#)
Ji Hwan Lim, Su Won Lee, Hoongyo Oh et al.
- [Film Boiling Heat Transfer from a Wire to Upward Flow of Liquid Hydrogen: Effect of Wire Diameter](#)
M Shiotsu, Y Shirai, T Matsumoto et al.



ECS
The
Electrochemical
Society
Advancing solid state &
electrochemical science & technology

DISCOVER
how sustainability
intersects with
electrochemistry & solid
state science research

Film boiling heat transfer from a wire to upward flow of liquid hydrogen and liquid nitrogen

M Shiotsu¹ Y Shirai¹ Y Horie¹ H Shigeta¹ D Higa¹ H Tatsumoto²
K Hata³ H Kobayashi⁴ S Nonaka⁴ Y Naruo⁴ and Y Inatani⁴

¹Dept. of Energy Sci. & Tech., Kyoto Univ., Sakyo-ku, Kyoto 606-8501, Japan

²J-PARC Center, Japan Atomic Energy Agency, Tokai, Ibaraki, 319-1195, Japan

³Inst. of Advanced Energy, Kyoto Univ., Uji, Kyoto 611-0011, Japan

⁴Inst. of Space and Astronautical Science, JAXA, Kanagawa, 229-8510, Japan

E-mail: shiotsu@pe.energy.kyoto-u.ac.jp

Abstract. Film boiling heat transfer coefficients in liquid hydrogen were measured for the heater surface superheats to 300 K under pressures from 0.4 to 1.1 MPa, liquid subcoolings to 11 K and flow velocities to 8 m/s. Two test wires were both 1.2 mm in diameter, 120 mm and 200 mm in lengths and were made of PtCo alloy. The test wires were located on the center of 8 mm and 5 mm diameter conduits of FRP (Fiber Reinforced Plastics). Furthermore film boiling heat transfer coefficients in liquid nitrogen were measured only for the 200 mm long wire. The film boiling heat transfer coefficients are higher for higher pressure, higher subcooling, and higher flow velocity. The experimental data were compared with a conventional equation for forced flow film boiling in a wide channel. The data for the 8 mm diameter conduit were about 1.7 times and those for the 5 mm conduit were about 1.9 times higher than the predicted values by the equation. A new equation was presented modifying the conventional equation based on the liquid hydrogen and liquid nitrogen data. The experimental data were expressed well by the equation.

1. Introduction

Knowledge of film boiling heat transfer from a heated wire to forced flow of liquid hydrogen or liquid nitrogen in a narrow gap is important for conductor design and quench analysis of superconducting magnets wound with high-T_c cable in conduit conductor (CICC). However there have been few experimental data as far as we know.

Shiotsu and Hama [1] studied the film boiling heat transfer from a vertical cylinder in forced flow of water and R113 in 40 mm dia. cylindrical conduit to make clear the heat transfer of reflooding process in a loss of coolant accident of a nuclear reactor. They derived a correlation of forced convection heat transfer.

Recently, Shiotsu et al. [2] have measured the forced convection film boiling heat transfer from a round wire to liquid hydrogen flowing upward in concentric annulus with a narrow gap. They reported that the experimental data were about 1.7 times higher than the values predicted by the Shiotsu-Hama equation, although the trend of dependence on flow velocity was similar to that predicted by the equation. They suggested that vapour film layer around the wire heater may be made thinner by a narrow gap.



The purpose of this study is firstly to obtain the experimental data of film boiling heat transfer from a heater wire to forced flow of liquid hydrogen and liquid nitrogen in round conduits with different gaps and secondly to present the film boiling heat transfer equation based on the experimental data.

2. Apparatus and method

Figure 1 shows a schematic of the experimental system, whose detail has been already presented in other paper [3]. It consists of a main cryostat, a sub tank (receiver tank), a connecting transfer tube with a control valve. Two test heater blocks are located in series at one end of the transfer tube in the main tank. They are used one by one. Liquid hydrogen in the main tank is forced to flow into the transfer tube by the pressure difference between the cryostat and sub tank. The mass flow rate is set by the pressure difference and the valve opening (CV001). Liquid hydrogen flows upward through the conduit of test heater blocks. The main tank is pressurized to a desired pressure by pure hydrogen gas (99.999 %) controlled by a gas regulator, while the sub tank is maintained to be atmospheric pressure. The mass flow rate is estimated by the weight change of the main tank, which is put on a scale (MettlerToledo WMHC 300s) that can measure up to 400 kg within 0.002 kg resolution. The feed hydrogen gas is controlled so that the pressure is kept constant during the test. Flow measurement error is estimated to be within 0.1 g/s. The inlet temperature T_B is measured by Cernox temperature sensor and controlled by a sheathed heater coil which is set at the bottom of the main tank.

Two types of test heater block are used. Type 1 has a test wire made of PtCo (0.5 wt. %) alloy, 1.2 mm in diameter, 120 mm in length supported at the centre of 8 mm diameter conduit in a block made of fibre reinforced plastic (FRP). Type 2 has a similar construction as shown in Figure 2. It has the test wire made of PtCo alloy, 1.2 mm in diameter, 195.3 mm in length supported at the centre of 5 mm diameter conduit. The heating current to the test wire is supplied by a power amplifier (max. 400 A at a power level of 4.8 kW). The input signal of the power amplifier is controlled so that the heat generation rate in the test wire agreed with a desired value. In this study, exponential heat generation rate of $Q = Q_0 e^{t/\tau}$ with $\tau = 10.0$ s up to a certain value Q_m at $t = t_m$ (at point E in figure 3), and $Q = Q_m e^{(t_m - t)/\tau}$ for $t > t_m$ are applied to the test wire. It was confirmed experimentally that the heat transfer phenomenon by

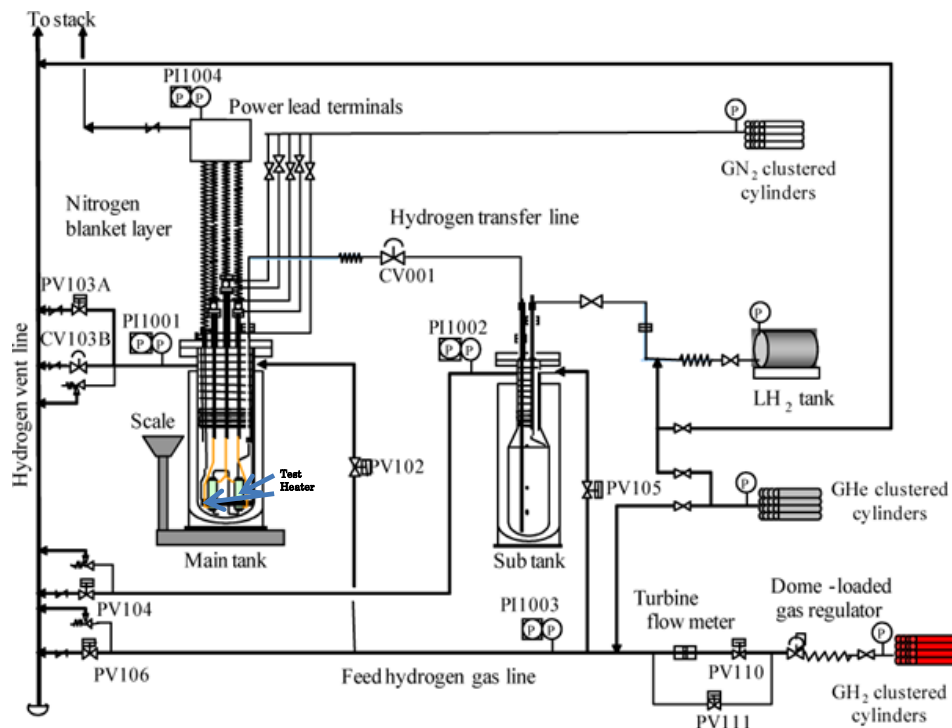


FIGURE 1. Schematic of the experimental apparatus.

this heat generation rate could be regarded as a continuous sequence of steady-state.

The electric resistance of the heater was measured. The voltage drops across the potential taps of the test wire and across a standard resistance and the output signal of a strain gauge pressure sensor were amplified and passed to a 16 bit digital memory system (Yokogawa WE7000). These signals are simultaneously sampled at 30 ms-intervals. The average temperature of the heated wire T_{av} was estimated using its electrical resistance. Temperature characteristics of the resistance had been obtained previously. The surface heat flux q was given as the difference between the heat generation rate Q and the time rate of energy storage. The average temperature on the heated surface T_w was calculated by solving steady-state conduction equation in a radial direction of the heater wire using T_{av} and Q (that is T_w is given as the boundary condition that satisfies measured T_{av} for Q).

The inlet temperature was measured by a Cernox sensor with an accuracy of 10 mK and amplified by a precision amplifier (Yokogawa 3131). Calibration of the measurement circuit is performed before a series of experiment by using a standard voltage-current generator and an approved pressure gauge. Experimental error is estimated to be within 1.0 K for T_w and 5 % for q , and 0.1 K for T_B .

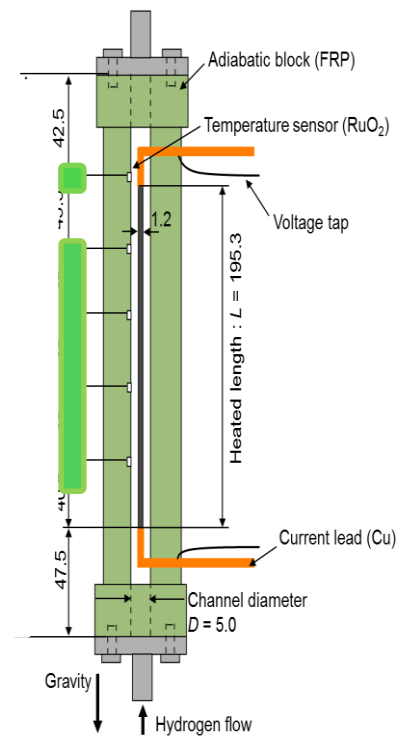


Figure 2 Type 2 test heater block.

3. Results and discussion

3.1 Typical heat transfer processes

Film boiling heat transfer coefficients were measured for the heater surface superheats up to 300 K under pressures from 0.4 to 1.1 MPa, liquid subcoolings to 11 K, and flow velocities to 8 m/s.

Figure 3 shows a typical process of a measured film boiling heat transfer without too much thermal shock to the test heater. Vertical axis is heat flux q and horizontal one is wall temperature increase from

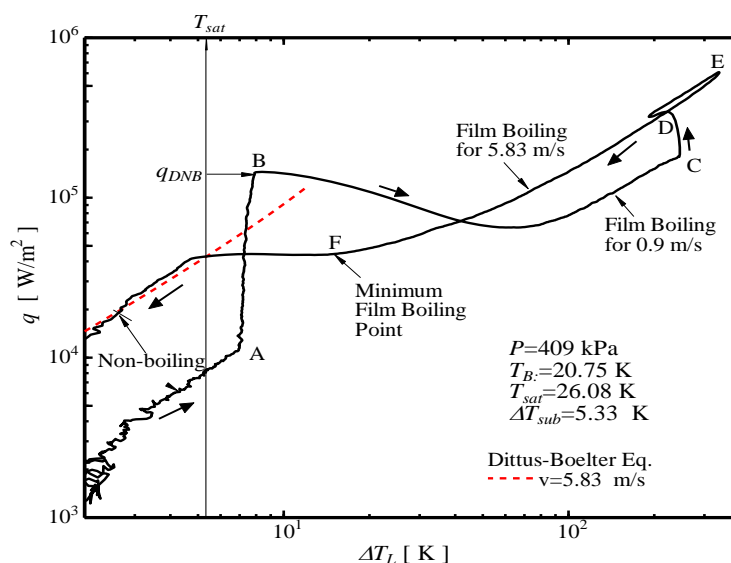


Figure 3 Heat transfer process to measure film boiling heat transfer.

inlet temperature. Firstly the heat generation rate was gradually increased for a low flow rate (0.9 m/s). Boiling initiates at point A. The process from A to B is nucleate boiling regime. When the heat flux reaches the DNB (Departure from Nucleate Boiling) heat flux (point B), heater temperature jumps to film boiling for 0.9 m/s (point C). Transient heat transfer process during the jump is shown in the figure. The process from B to the bottom of heat flux is the transition boiling and the bottom to the point C is film boiling. Then flow velocity is increased to a desired value (here 5.83 m/s) while heating current is continuously increased to the heater temperature around 300 K. Then the heating current is decreased exponentially and film boiling heat transfer coefficients are measured.

3.2 Results of film boiling heat transfer in liquid hydrogen

Figure 4 and figure 5 show the relations between film boiling heat transfer coefficient $h = q / \Delta T_{sat}$ versus wall superheat ΔT_{sat} at $P = 0.4$ MPa under saturated condition with flow velocity as a parameter for the Type 1 and Type 2 heaters, respectively. Broken lines in these figures are the predicted curves by our correlation shown later. As the heat input is reduced from high ΔT_{sat} (the fully developed film boiling regime) down to about 80 K, the coefficient h decreases gradually, however, for further decrease of wall superheat ΔT_{sat} , that is heat input, the coefficient h increases steeply, since the vapor film becomes thinner drastically. The film boiling heat transfer coefficients are higher for higher flow velocity.

The length z and the equivalent diameter D_e of the Type 2 heater are about 1.63 times and 0.56 times as long as those of Type 1, respectively. It can be seen from the comparison of the heat transfer coefficients for the Type 1 and Type 2 heaters for nearly the same velocities such as 1.6 m/s and 1.98 m/s, and 4.1 m/s and 4.71 m/s that they are almost same. This would be due to combined effects of heater length and equivalent diameter. The heat transfer coefficients would be lower for longer heater length due to the growth of vapor film along the heater. The heat transfer coefficients would be higher for smaller equivalent diameter because vapour film layer around the wire heater would be made thinner by a narrower gap.

The experimental data for the lowest velocities of 0.77 m/s and 1.98 m/s in figures 4 and 5, respectively, could not be obtained for ΔT_{sat} higher than approximately 180 K. The flow velocity was so small that the hydrogen flow could not keep the designated velocity in higher wall superheat.

Figures 6 and 7 show the relations between film boiling heat transfer coefficient and ΔT_{sat} for the Type 2 heater at $P = 0.7$ MPa under saturated condition and liquid subcooling of 8 K with flow velocity as a parameter. Trend of the dependence on ΔT_{sat} and flow velocity is similar to that for saturated

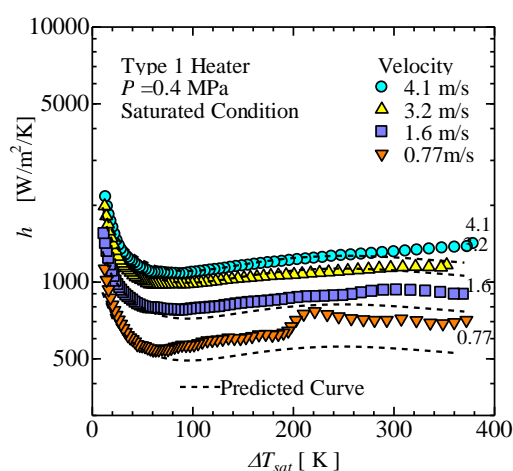


Figure 4 Film boiling heat transfer coefficients for Type 1 heater at $P=0.4$ MPa under saturated condition.

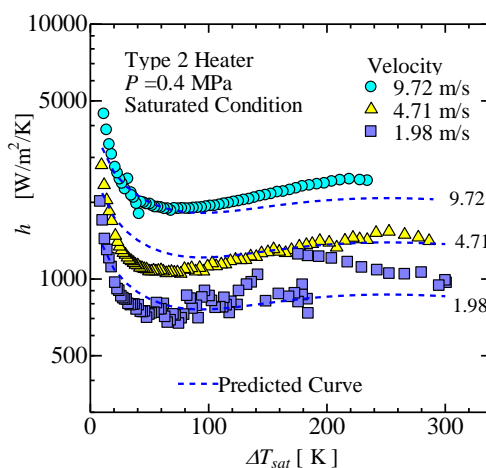


Figure 5 Film boiling heat transfer coefficients for Type 2 heater at $P=0.4$ MPa under saturated condition.

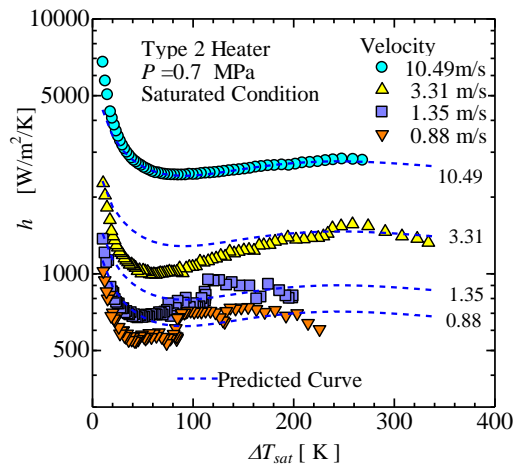


Figure 6. Film boiling heat transfer coefficients for Type 2 heater at $P=0.7$ MPa under saturated condition.

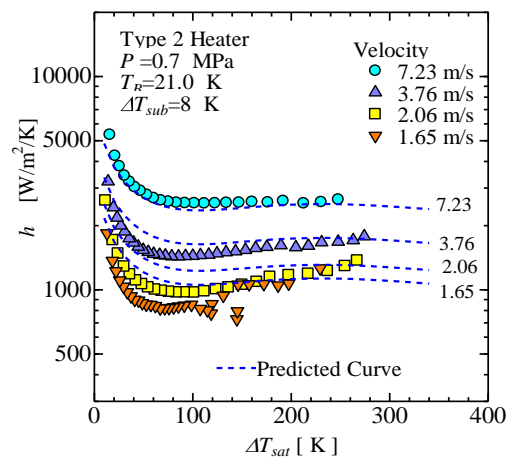


Figure 7. Film boiling heat transfer coefficients for Type 2 heater at $P=0.7$ MPa for $\Delta T_{sub}=8$ K.

condition mentioned above. By comparing the data for 9.72 m/s in figure 5 with that for 10.49 m/s in figure 6 and the data for 3.31 m/s in figure 6 with that for 3.76 m/s in figure 7, we can see that the heat transfer coefficients are higher for higher pressure and liquid subcooling.

3.3 Results of film boiling heat transfer in liquid nitrogen

Forced flow film boiling heat transfer coefficients of liquid nitrogen were measured for $P = 0.55$ and 1.0 MPa using the same apparatus and experimental procedure.

Figures 8 and 9 show the results for the Type 2 heater in forced flow of liquid nitrogen. The heat transfer curves in the figures are for the inlet temperature of 78 K ($\Delta T_{sub} = 16$ K) at $P = 0.55$ MPa and at 1.0 MPa ($\Delta T_{sub} = 25$ K), respectively. Broken lines in the figures are the predicted values by our correlation described later. As the viscosity of liquid nitrogen is about 15 times higher than liquid hydrogen, maximum flow velocity attained for the Type 2 test heater is far lower than that for liquid hydrogen. Though in a narrow range, effect of flow velocity is clearly seen in these figures; film boiling heat transfer coefficients are higher for higher flow velocity.

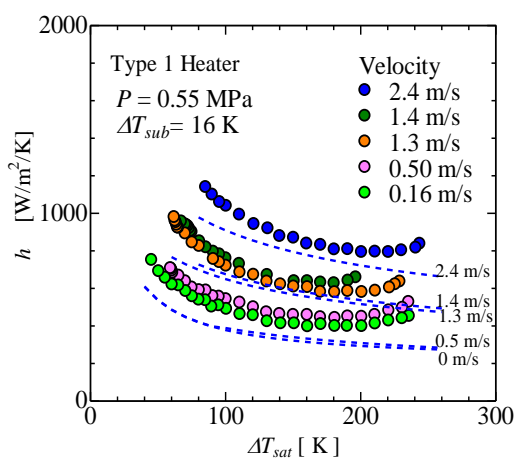


Figure 8 Film boiling heat transfer in liquid nitrogen for Type 1 heater at 0.55 MPa.

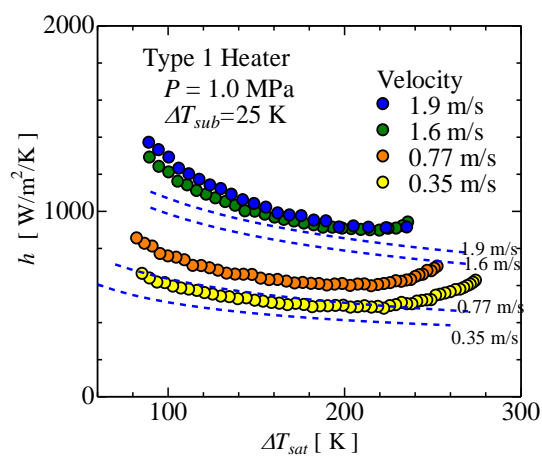


Figure 9 Film boiling heat transfer in liquid nitrogen for Type 1 heater at 1.0 MPa.

4. Film boiling correlation

4.1 Derivation of the correlation

Recently, we [2] have measured the forced convection film boiling heat transfer from a round wire to liquid hydrogen flowing upward in concentric annulus with a narrow gap. We found that the experimental data were about 1.7 times higher than the values predicted by the Shiotsu-Hama equation [1], although the trend of dependence on flow velocity was similar to that by the equation.

Shiotsu-Hama equation was based on the experimental data for a wide conduit. We have assumed that the vapour film layer around the wire heater would be made thinner by a very narrow gap. By introducing the equivalent diameter D_e to express the gap effect, we have derived the following equation by extending the Shiotsu-Hama equation based on the experimental data of hydrogen and nitrogen obtained in this work.

$$\overline{Nu}_{D_e} = 0.63(zD_e^{-1})^{-1/4} Re_{D_e}^{0.55} (\mu_l \mu_v^{-1}) M^{-1/3} F_p \quad \text{for } Re_{D_e} \geq F_v \quad (1)$$

where

$$M = (SpR^{-2})[1 + \{E_2(2Pr_l Sp)^{-1}\}][1 - 0.7ScE_2^{-1}] \quad (2)$$

$$F_p = 1.0 + 0.7(PP_{cr}^{-1})^{0.9} \quad (3)$$

E_2 is a positive root of the following cubic equation.

$$E_2^3 + (5Pr_l Sp - Sc)E_2^2 - 5Pr_l Sp Sc E_2 - 7.5Pr_l^2 Sp^2 R^2 = 0 \quad (4)$$

The film boiling heat transfer coefficients predicted by Eq. (1) decrease with the decrease in flow velocity but do not become lower than the coefficients of pool film boiling heat transfer from a vertical surface given by the following equation [4].

$$\overline{Nu}_{D_e} = 0.52(z^{-1}D_e) \left[z \{g(\rho_l - \rho_v)\sigma^{-1}\}^{1/2} \right]^{1/4} M_z^{1/4} \quad \text{for } Re_{D_e} < F_v \quad (5)$$

where

$$M_z = Gr_z Sp^{-1} E^3 \left\{ 1 + E (Sp Pr_l)^{-1} \right\}^{-1} (R Pr_l Sp)^{-2} \quad (6)$$

$$E = \left(A + CB^{1/2} \right)^{1/3} + \left(A - CB^{1/2} \right)^{1/3} + (1/3)Sc^* \quad (7)$$

$$A = (1/27)Sc^{*3} + (1/3)R^2 Sp Pr_l Sc^* + (1/4)R^2 Sp^2 Pr_l^2 \quad (8)$$

$$B = (-4/27)Sc^{*2} + (2/3)Sp Pr_l Sc^* - (32/27)Sp Pr_l R^2 + (1/4)Sp^2 Pr_l^2 + (2/27)Sc^{*3}/R^2 \quad (9)$$

$$C = 0.5R^2 Sp Pr_l \quad (10)$$

$$Sc^* = 0.93Pr_l^{0.22} Sc \quad (11)$$

The lower limit, F_v , of Re number for equation (1) is given as follows by equating equation (1) with equation (2).

$$F_v = 0.71(z^{-1}D_e)^{1.364} \left[z \{g(\rho_l - \rho_v)\sigma^{-1}\}^{1/2} \right]^{0.455} M_z^{0.455} (\mu_v \mu_l^{-1})^{1.818} M^{0.606} F_p^{-1.818} \quad (12)$$

4.2 Comparison with the experimental data

The film boiling heat transfer coefficients predicted by equations (1) and (5) are compared with the data of liquid hydrogen in figures 4 to 7 and with the data of liquid nitrogen in figures 8 and 9. We can see that the trend of dependence on wall superheat and flow velocity at each pressure and subcooling are expressed well by the equation. In case of liquid nitrogen, the prediction accuracy is not as good as that for liquid hydrogen. The equation underestimates the experimental data especially for the flow velocities lower than 1 m/s.

To see the applicability of the correlation in more detail, all the experimental data of liquid hydrogen under saturated and subcooled conditions at pressures for the Type 1 and Type 2 heaters except those for $Re_{De} < F_c$ are shown on $\overline{Nu}_{De}(\mu_v/\mu_l)M^{1/3}(z/D_e)^{1/4}F_p^{-1}$ vs. Re_{De} graph in figure 10. The curve of equation (1) is shown in the figure as a straight line. The error bands of $\pm 20\%$ are shown as dotted lines. We can see that most of the experimental data are within $\pm 20\%$ of the values predicted by the equation

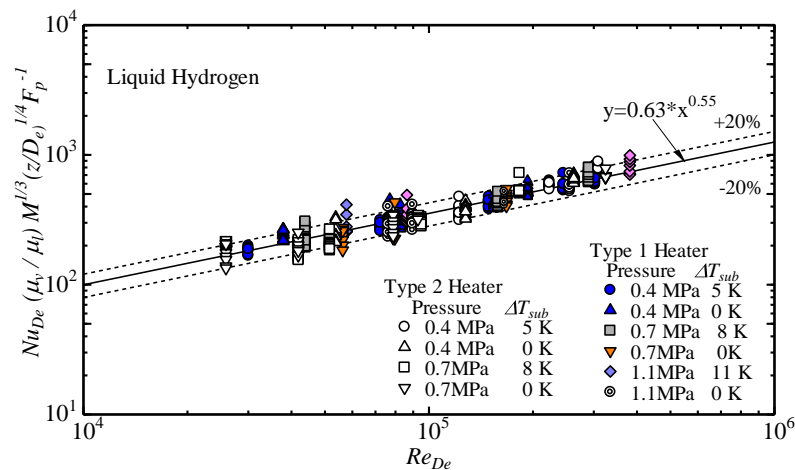


FIGURE 10. Comparison of the correlation with the experimental data of liquid hydrogen

4.3 Comparison with the conventional non-cryogenic data

The experimental data of water under saturated condition and R113 under subcooled condition by Shiotsu and Hama [1] are shown in Figures 11 and 12. The curves of equations (1) and (5) are also shown in these figures. The values predicted by our equation for each flow velocity agree with the experimental data of water and R113 with $\pm 10\%$ error. It is expected that our correlation can express film boiling heat transfer in forced flow of cryogenic and non-cryogenic liquids for a round wire in conduits with various gaps, although further study is necessary for confirmation.

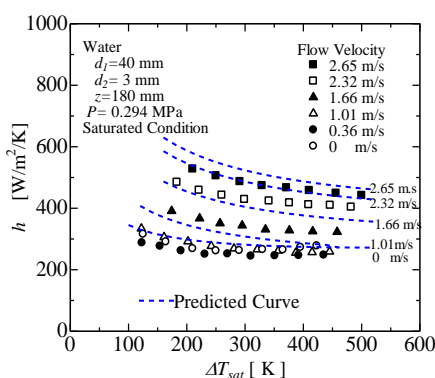


Figure 11. Comparison of our correlation with water data [1] for 40 mm-dia. conduit.

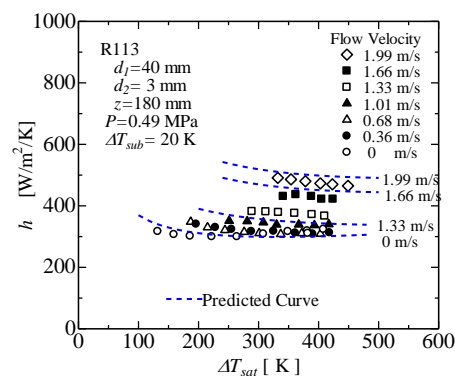


Figure 12. Comparison of our correlation with R113 data [1] for 40 mm-dia. conduit.

5. Conclusions

Film boiling heat transfer coefficients were measured for the two types of heater blocks with the same diameter of the heater wire and different heater lengths and gaps of the conduit. The experimental results led to the following conclusions.

The heat transfer coefficients are higher for higher pressure, higher subcooling and higher flow

velocity.

The heat transfer coefficients for the Type 1 and Type 2 heaters for nearly the same velocities are almost the same, though the length z and the equivalent diameter D_e of the Type 2 heater are about 1.6 times and 0.56 times as long as those of Type 1, respectively.

A new correlation was presented modifying the Shiotsu-Hama equation by introducing the equivalent diameter D_e to express the gap effect.

The experimental data of liquid hydrogen and liquid nitrogen are expressed well by the new correlation.

The experimental data of water and R113 by Shiotsu and Hama [1] are also expressed well by the new correlation. It is expected that our correlation can express film boiling heat transfer in forced flow of cryogenic and non-cryogenic liquids for a round wire in conduits with various gaps, although further study is necessary for confirmation.

6. Acknowledgments

This research was supported in part by JST, ALCA. The authors thank the technical staffs of JAXA for their technical assistance.

7. References

- [1] Shiotsu M and Hama K 2000 *Nucl. Eng. & Des.* **200** 23
- [2] Shiotsu M *et al* 2015 *Physics Procedia* **87** 631.
- [3] Tatsumoto H *et al* 2010 *J. Physics Conference Series* 234.
- [4] Sakurai A *et al* 1992 *Pool Film Boiling Heat Transfer and Minimum Film Boiling Temperature in Pool and External Flow Boiling* ed by V K Dhir and A E Bergles ASME pp277-301

8. Nomenclature

| | | | |
|-----------------------|---|------------------|---|
| D_e | :(= $d_1 - d_2$), equivalent diameter, (m) | superheat | |
| d_1 | :inner diameter of conduit (m) | T_{av} | :average heater temperature (K) |
| d_2 | :heater diameter (m) | T_B | :inlet liquid temperature (K) |
| Gr_z | :(= $g(\rho_l - \rho_v)\rho_v^{-1}z^3\nu_l^{-2}$), Grashof number | T_{sat} | :saturation temperature (K) |
| h | :(= $q / \Delta T_{sat}$), boiling heat transfer coefficient ($\text{Wm}^{-2}\text{K}^{-1}$) | T_w | :heater surface temperature (K) |
| h_{fg} | :latent heat (Jkg^{-1}) | u | :flow velocity (ms^{-1}) |
| h'_{fg} | :(= $h_{fg} + 0.5c_{pv}\Delta T_{sat}$), modified latent heat (Jkg^{-1}) | z | :test heater length (m) |
| \overline{Nu}_{D_e} | :(= hD_e / λ_v), average Nusselt number | ΔT_{sat} | :(= $T_w - T_{sat}$), surface superheat (K) |
| P | :pressure (kPa) | ΔT_{sub} | :(= $T_{sat} - T_B$), subcooling (K) |
| P_{cr} | :critical pressure (kPa) | λ | :thermal conductivity ($\text{Wm}^{-1}\text{K}^{-1}$) |
| Pr_l | :(= $c_{pl}\mu_l / \lambda_l$), Prandtl number of liquid | μ | :viscosity ($\text{kg s}^{-1}\text{m}^{-1}$) |
| Pr_v | :(= $c_{pv}\mu_v / \lambda_v$), Prandtl number of vapor | ν | :kinematic viscosity (m^2s^{-1}) |
| Q | :heat generation rate (Wm^{-3}) | ρ | :density (kgm^{-3}) |
| q | :heat flux (Wm^{-2}) | σ | :surface tension (Nm^{-1}) |
| R | :(= $\{\rho_v\mu_v / (\rho_l\mu_l)\}^{1/2}$) | τ | :exponential period (s) |
| Re_{D_e} | :(= uD_e / ν_l), Reynolds number | Subscripts | |
| Sc | :(= $c_{pl}\Delta T_{sub} / h'_{fg}$), non-dimensional subcooling | l | : liquid, |
| Sp | :(= $c_{pv}\Delta T_{sat} / h'_{fg} / Pr_v$), non-dimensional | v | :vapor |